Standing-wave excited soft x-ray photoemission microscopy: Application to Co microdot magnetic arrays

Alexander X. Gray,[1,2,a] Florian Kronast,[3] Christian Papp,[2,4] See-Hun Yang,[5] Stefan Cramm,[6] Ingo P. Krug,[6] Farhad Salmassi,[7] Eric M. Gullikson,[7] Dawn L. Hilken,[7] Erik H. Anderson,[7] Peter Fischer,[2] Hermann A. Dürr,[3] Claus M. Schneider,[6] and Charles. S. Fadley[1,2]

[1]*Department of Physics, University of California, Davis, California 95616, USA*
[2]*Material Sciences Division, Lawrence Berkeley National Laboratory, Berkeley, California 94720, USA*
[3]*Helmholtz-Zentrum Berlin, Albert-Einstein-Straße 15, 12489 Berlin, Germany*
[4]*Lehrstuhl für Physikalische Chemie II, Universität Erlangen-Nürnberg, Egerlandstraße 3, D-91054 Erlangen, Germany*
[5]*IBM Almaden Research Center, San Jose, California 95120, USA*
[6]*Institute of Solid State Research IFF-9, Research Center Jülich, Jülich D-52425, Germany*
[7]*Center for X-Ray Optics, Lawrence Berkeley National Laboratory, Berkeley, California 94720, USA*

(Received 6 April 2010; accepted 18 July 2010; published online 10 August 2010)

We demonstrate the addition of depth resolution to the usual two-dimensional images in photoelectron emission microscopy (PEEM), with application to a square array of circular magnetic Co microdots. The method is based on excitation with soft x-ray standing-waves generated by Bragg reflection from a multilayer mirror substrate. Standing wave is moved vertically through sample simply by varying the photon energy around the Bragg condition. Depth-resolved PEEM images were obtained for all of the observed elements. Photoemission intensities as functions of photon energy were compared to x-ray optical calculations in order to quantitatively derive the depth-resolved film structure of the sample. © *2010 American Institute of Physics*. [doi:10.1063/1.3478215]

Soft x-ray photoelectron emission microscopy (PEEM) is an established powerful technique, enabling element-specific studies of surfaces and nanostructures through images obtained via core-level excitations of photoelectrons and secondary electrons. PEEM has been used extensively in recent years to study element-specific physical, chemical, structural, and magnetic properties of surfaces, resulting in a plethora of literature revealing interesting surface and nanostructure phenomena.[1–6] Most of these studies involve image formation from low-energy secondary electrons, although a growing number of microscopes can image with an energy-resolved photoelectron or Auger intensity that is thus also element-specific. PEEM images to date are inherently two-dimensional in space, with resolutions in the lateral x and y directions that are now typical 10–20 nm but which promise in the future to be in the few nanometer regime.[7]

Very recently, a method has been suggested, by which soft x-ray standing-wave excitation extends the dimensionality of the PEEM, giving this technique depth resolution.[8] This depth resolution is achieved by setting-up an x-ray standing wave (SW) field in the sample by growing it on a synthetic periodic multilayer mirror substrate which in first-order Bragg reflection acts as the SW-generator.[9] The SW can then be moved vertically through the sample in several following ways: by varying the photon energy or the incidence angle through the Bragg condition, or in a previous study of this type, also by growing one layer of the sample as a wedge and looking along the wedge.[8] As the antinodes of the electromagnetic field shift vertically through the sample, they highlight various parts of the sample, introducing depth-selectivity in the photoemission process. Exploiting this depth-selectivity in an element-specific way requires an energy-selection of photoelectrons contributing to the PEEM image so as to image with a given core-electron intensity. In a previous exploratory study, this SW-PEEM technique has been used to determine the depth-resolved properties of a Ag-wedge/Co/Au multilayer nanostructure.[8] It was shown that with a suitable wedge-profile sample, the vertical resolution in the PEEM images approaches $\sim \pm 3-4$ Å and is thus about 1/10 of the SW period, which is in turn equal to the period of the multilayer of 3–4 nm.

In this study, we demonstrate the next step in the SW-PEEM approach; imaging a lateral array of microstructures with depth resolution, as a prelude to future applications with true nanometer resolution in three dimensions. In contrast with the previous study[8] the approach used here, namely, moving the SW through the structure by means or varying photon energy, is simpler and more versatile because it does not require one to grow the layer of interest in a shape of a wedge. Due to this improvement, it is possible to measure patterned structures which are more technologically relevant, such as arrays of microdots or pillars described in this paper.

One of the major advantages of the SW-PEEM technique is the enhanced interface-sensitivity of the measurement due to the possibility of translating the antinodes of the SW vertically through the sample and therefore choosing the "epicenter" of the photoemission. This effect cannot be achieved with other methods, such as, for example, using harder x-rays in order to increase the probing depth.

We have investigated a nanostructured system consisting of square arrays of circular magnetic cobalt microdots, nominally 4 nm in thickness and 1 μm in diameter, grown on a multilayer substrate of configuration [23.6 Å-Si/15.8 Å-Mo]$\times$40, as depicted in cross section in

[a]Electronic mail: agray@ucdavis.edu.

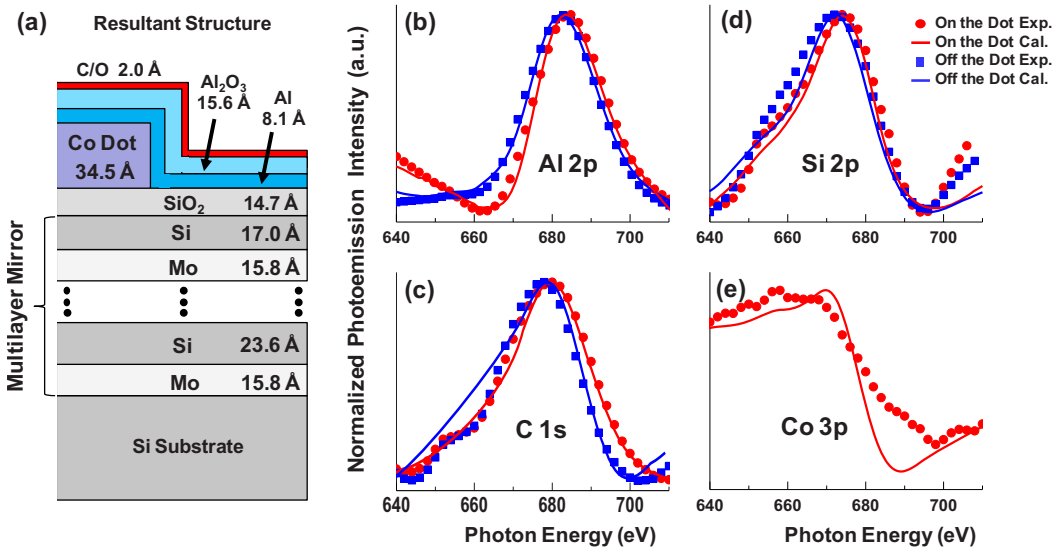

FIG. 1. (Color online) (a) Self-consistent model of the film structure obtained as the result of simultaneous fitting of all the scanned-energy curves in (b), (c), (d), and (e). Experimental (data points) and calculated (solid curves) results of photoemission intensity as functions of photon energy with the electron kinetic energy for imaging set to (b) Al 2*p*, (c) C 1*s*, (d) Si 2*p*, and (e) Co 3*p* core levels.

Fig. 1(a). Protection against oxidation of the Co and Si surfaces was provided by a 2-nm-thick aluminum cap layer. The samples were fabricated at the Center for X-Ray Optics at the Lawrence Berkeley National Laboratory. The surface carbon contamination has been removed from the Si/Mo multilayer prior to the deposition of the microdots and the capping layer. The core-level photoemission peaks used in the element-specific study of the constituents of the structure are indicated in [Figs. 1(b)–1(e)]. The C 1*s* core-level signal originated from the thin carbon-containing overlayer covering the sample after removal from the growth chamber and exposure to ambient contaminants.

The experiment was conducted at the elliptically polarized microfocus soft x-ray undulator beamline UE49-PGM-a at the storage ring BESSY-II (Helmholtz Zentrum Berlin), equipped with the Elmitec PEEM-II endstation with an integrated photoelectron energy analyzer.[10]

Simulations of expected spectra were performed using the NIST DATABASE software; simulation of electron spectra for surface analysis.[11] The results indicated that a combination of the photon energy of 663 eV and a grazing angle of 13.8° would yield the most cleanly resolvable Co 3*p*, Al 2*p*, Si 2*p*, and C 1*s* photoemission spectra, unobstructed by any Auger electron features. The grazing incidence angle which satisfies the Bragg condition is found experimentally in a matter of minutes via a simple core-level photoemission intensity rocking-curve measurement.

The x-ray beam was focused into a small spot of ~10 μm in cross section, comparable with the dimensions of several periods in the Co microdot array. The spot was chosen smaller than the field of view in the microscope and is unavoidably elongated in the horizontal direction by about a factor of 3.5 due to the grazing incidence geometry [cf. Figs. 2(a)–2(d)]. All measurements were conducted in a normal photoemission geometry with the incidence angle fixed at 13.8° and the photon energy was varied between 620 and 750 eV in order to scan the SW generated by the multilayer substrate vertically through the structure.

Figures 1 and 2 summarize our results, with the data points in Figs. 1(b)–1(e) depicting the photoemission intensities for four core-level photoemission peaks—Al 2*p*, C 1*s*, Si 2*p*, and Co 3*p*—as functions of photon energy and therefore as functions of the vertical position of the SW in the sample. Photoemission peak intensities in images based on these four peaks, as shown in Fig. 2, were extracted from the areas inside and outside of the Co microdots using specialized image-processing software, background subtracted and normalized.[12]

The shapes of the photoemission intensity profiles versus photon energy [Figs. 1(b)–1(e)] contain detailed information about the vertical dimensions of each layer in the sample. We used the x-ray optical simulation software developed by S.-H. Yang[13] to model the photoemission intensities for the Al 2*p*, C 1*s*, Si 2*p*, and Co 3*p* core levels as a function of photon energy at our fixed incidence angle of 13.8° and a

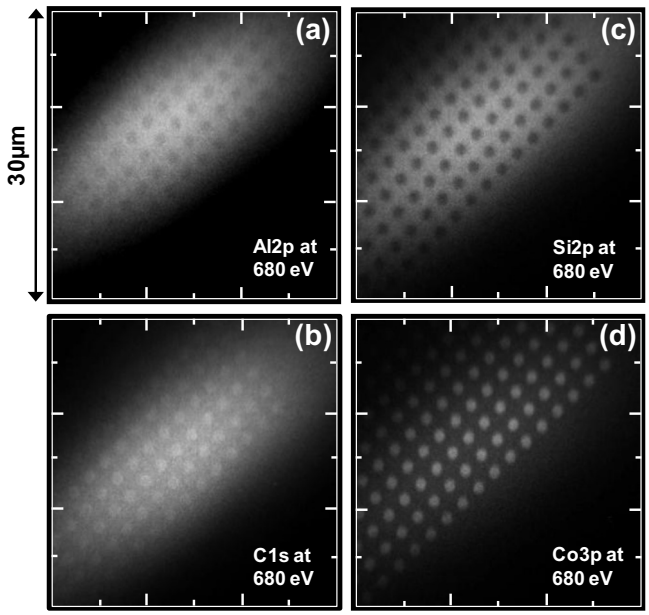

FIG. 2. Standing-wave PEEM images captured at $h\upsilon = 680$ eV, for (a) Al 2*p*, (b) C 1*s*, (c) Si 2*p*, and (d) Co 3*p* core levels. 680 eV is the energy for which the Al image is a maximum off the microdots.

normal photoemission geometry. The software uses x-ray optical theory based on Maxwell's equations in order to calculate the intensity of the electric field inside and outside the sample, and then calculates photoemission intensities for any core level as functions photon energy, as well as incidence and take-off angles, while taking into account subshell photoelectric cross sections as well as inelastic mean-free paths of the electrons. The ultimate goal of the x-ray optical simulation was to obtain a self-consistent model of the sample with a single set of layer thicknesses. The model should not only quantitatively describe the vertical dimensions of the entire film structure, in the lateral on-dot and off-dot regions but also simultaneously fit all of the experimental photoemission intensity profiles (data points). The final determined structure is shown in Fig. 1(a) and the theoretical results based upon it are shown as solid lines in Figs. 1(b)–1(e). The agreement is in general excellent, not just as to the positions along the photon energy scale but also as to the shapes of the photoemission intensity profiles. In addition, almost all of the differences on-dot and off-dot were reproduced with striking similarity using the single model depicted in Fig. 1(a).

The model indicates that the top Si layer of the Si/Mo multilayer substrate is covered with a 14.7 Å layer of SiO_x, mostly SiO_2, resulting from the exposure of the multilayer to air before microdot deposition. The remaining Si layer is only 17.0 Å thick, which means that 6.6 Å of Si was consumed by the SiO_x film as a result of the oxidation. Since the number density of Si atoms in pure Si is 5.00×10^{22} g^{-1} and the same value for SiO_2 is 2.24×10^{22} g^{-1}, for every one Ångstrom of pure Si consumed by the oxidation, 5.00/2.24 =2.23 Å of SiO_2 is created. Therefore, the value of 14.7 Å of SiO_x is consistent with conserving the number of Si atoms in Si-surface oxidation. The thickness of the Co microdots was determined to be 34.5 Å, instead of the nominal value of 40 Å. This value is consistent with the growers' prediction of ~20% in process variation for Co growth. The Al capping layer was found to be partially oxidized, leaving 8.1 Å of pure Al and 15.6 Å of AlO_x, mostly as Al_2O_3, as derived by a self-consistent conservation of the number of Al atoms involved in Al-surface oxidation. Thickness of the overlying carbon-containing layer was determined to be 2.0 Å.

The qualitative differences in images shown in Fig. 2 for the four peaks are also easy to understand. These images were all obtained with a photon energy of 680 eV, the energy at which the maximum in the intensity of the Al 2*p* line occurs for the aluminum atoms around the dots [Fig. 2(a)]. This phenomenon occurs because at the photon energy of 680 eV an antinode of the SW is situated at the vertical position of the valleys below the Co microdots. In case of the C 1*s* photoemission peak, the microscope image captured at the photon energy of 680 eV highlights the carbon atoms on top of the Co microdots [Fig. 2(b)]. This happens because at the photon energy of 680 eV another antinode of the SW is situated at the vertical position of the carbon-containing surface contaminant layer on top of the Co microdots. For the Si 2*p* core level, Fig. 2(c) shows that the photoemission intensity "on the dots" is significantly damped, since the Si atoms are buried beneath the surface by the 4-nm-thick Co microdots. The intensity of the main pure Si 2*p* peak, rather than the Si 2*p* oxide peak, was used for the Si image. Finally, for the Co 3*p* image in Fig. 2(d), due to the absence of cobalt in the valleys between the dots, the microscopy image shows zero-intensity for the areas off the dots.

The application of scanned-energy standing-wave excited soft x-ray photoemission microscopy to the depth-resolved imaging of Co magnetic microdot arrays was investigated. It was shown that this technique can be used to produce element-specific and depth-sensitive images of such patterned samples. In conjunction with x-ray optical theoretical modeling, quantitative information about the depth-dependent chemical composition of the sample can be extracted from the photoemission data. The good agreement between our experimental results and model calculations suggests that future studies with better spatial and spectral resolution will also yield more detailed information about the interfacial regions. In addition, exploiting magnetic dichroism in core-level photoemission with circularly[14] and linearly polarized light[15,16] will introduce magnetic sensitivity into the technique, resulting in a unique approach for complex magnetic thin-film nanostructures. This addition of quantitative depth sensitivity to the conventional laterally resolved soft x-ray PEEM thus should considerably enhance the capabilities of the PEEM as a research, development and metrology tool for science and industry.

The authors acknowledge support from the Director, Office of Science, Office of Basic Energy Sciences, Materials Sciences, and Engineering Division, of the U.S. Department of Energy under contract number DE-AC02-05CH11231.

[1]S. Anders, H. A. Padmore, R. M. Duarte, T. Renner, T. Stammler, A. Scholl, M. R. Scheinfein, J. Stöhr, L. Séve, and B. Sinkovic, Rev. Sci. Instrum. **70**, 3973 (1999).
[2]E. Bauer, J. Electron Spectrosc. Relat. Phenom. **114–116**, 975 (2001).
[3]C. M. Schneider and G. Schönhense, Rep. Prog. Phys. **65**, 1785 (2002).
[4]A. Gloskovskii, J. Barth, B. Balke, G. H. Fecher, C. Felser, F. Kronast, R. Ovsyannikov, H. Dürr, W. Eberhard, and G. Schönhense, J. Phys. D **40**, 1570 (2007).
[5]B. Heitkamp, F. Kronast, L. Heyne, H. A. Dürr, W. Eberhardt, S. Landis, and B. Rodmacq, J. Phys. D **41**, 164002 (2008).
[6]C. Boeglin, O. Ersen, M. Pilard, V. Speisser, and F. Kronast, Phys. Rev. B **80**, 035409 (2009).
[7]R. Fink, M. R. Weiss, E. Umbach, D. Preikszas, H. Rose, R. Spehr, P. Hartel, W. Engel, R. Degenhardt, R. Wichtendahl, H. Kuhlenbeck, W. Erlebach, K. Ihmann, R. Schlögl, H.-J. Freund, A. M. Bradshaw, G. Lilienkamp, T. Schmidt, E. Bauer, and G. Benner, J. Electron Spectrosc. Relat. Phenom. **84**, 231 (1997).
[8]F. Kronast, R. Ovsyannikov, A. Kaiser, C. Wiemann, S. H. Yang, D. E. Burgler, R. Schreiber, F. Salmassi, P. Fischer, H. A. Durr, C. M. Schneider, W. Eberhardt, and C. S. Fadley, Appl. Phys. Lett. **93**, 243116 (2008).
[9]S.-H. Yang, B. S. Mun, N. Mannella, S.-K. Kim, J. B. Kortright, J. Underwood, F. Salmassi, E. Arenholz, A. Young, Z. Hussain, M. A. V. Hove, and C. S. Fadley, J. Phys.: Condens. Matter **14**, L407 (2002).
[10]F. Kronast, R. Ovsyannikov, H. A. Dürr, and W. Eberhardt, "A high resolution soft x-ray photoelectron emission microscope with integrated spin analysis" (unpublished).
[11]W. Smekal, W. S. M. Werner, and C. J. Powell, Surf. Interface Anal. **37**, 1059 (2005).
[12]See supplementary material at http://dx.doi.org/10.1063/1.3478215 for details on background subtraction.
[13]S.-H. Yang, "Soft x-ray optics in XPS, AES and XES" (unpublished).
[14]L. Baumgarten, C. M. Schneider, F. Schäfers, H. Petersen, and J. Kirschner, Phys. Rev. Lett. **65**, 492 (1990).
[15]R. Schellenberg, E. Kisker, A. Fanelsa, F. U. Hillebrecht, J. G. Menchero, A. P. Kaduwela, C. S. Fadley, and M. A. v. Hove, Phys. Rev. B **57**, 14310 (1998).
[16]C. Roth, F. U. Hillebrecht, H. B. Rose, and E. Kisker, Phys. Rev. Lett. **70**, 3479 (1993).